

JGR Solid Earth

RESEARCH ARTICLE

10.1029/2019JB017795

Key Points:

- Anomalous long duration of long-period ground motions was observed during seismic wave propagation from the 2016 *M*7.8 Kaikoura earthquake
- Waveform modeling indicates the presence of a thick, unusually low seismic-velocity wedge of material in the northeastern North Island of NZ
- Long-duration ground motions caused by this wedge would enhance dynamic triggering of slow slip as well as hazard posed by ground shaking

Supporting Information:

- Supporting Information S1

Correspondence to:

Y. Kaneko,
y.kaneko@gns.cri.nz

Citation:

Kaneko, Y., Ito, Y., Chow, B., Wallace, L. M., Tape, C., Grapenthin, R., et al. (2019). Ultralong duration of seismic ground motion arising from a thick, low-velocity sedimentary wedge. *Journal of Geophysical Research: Solid Earth*, 124. <https://doi.org/10.1029/2019JB017795>

Received 3 APR 2019

Accepted 28 AUG 2019

Accepted article online 2 SEP 2019

Ultra-long Duration of Seismic Ground Motion Arising From a Thick, Low-Velocity Sedimentary Wedge

Yoshihiro Kaneko¹ , Yoshihiro Ito² , Bryant Chow³, Laura M. Wallace^{1,4} , Carl Tape⁵ , Ronni Grapenthin^{6,7} , Elisabetta D'Anastasio¹ , Stuart Henrys¹ , and Ryota Hino⁸

¹GNS Science, Lower Hutt, New Zealand, ²Disaster Prevention Research Institute, Kyoto University, Kyoto, Japan,

³School of Geography, Environment and Earth Sciences, Victoria University of Wellington, Wellington, New Zealand,

⁴Institute for Geophysics, University of Texas at Austin, Austin, TX, USA, ⁵Geophysical Institute, University of Alaska Fairbanks, Fairbanks, AK, USA, ⁶Geophysics at the Earth & Environmental Science Department, New Mexico Institute of Mining and Technology, Socorro, NM, USA, ⁷Now at Geophysical Institute, University of Alaska Fairbanks, Fairbanks, AK, USA, ⁸International Research Institute of Disaster Science, Tohoku University, Sendai, Japan

Abstract Sedimentary basins are known to amplify and increase the duration of ground motions that accompany earthquakes. A similar phenomenon is expected, but not as well documented, in low seismic-velocity accretionary prisms along subduction margins. In this study, we report anomalously long duration of long-period ground motions observed in the North Island of New Zealand during seismic wave propagation from the *M*7.8 Kaikoura earthquake ~600 km away. Unique waveform data captured by strong-motion, high-rate GPS and ocean bottom pressure sensors reveal that long-period ground motions lasted longer than 450 s in the northeastern North Island. These waveforms indicate one of the longest durations of long-period (>10 s) ground motions ever recorded at similar epicentral distances for comparable, large earthquakes. To understand the underlying mechanism, we use numerical simulations of seismic wave propagation. We find that a velocity model that includes an accretionary prism, modeled as a large-scale (~30,000 km²) wedge characterized by extremely low seismic wave speeds, can explain the observed long durations of long-period ground motions as the reverberations of seismic waves within the low-velocity wedge. We show that the long duration of long-period ground motions leads to prolonged dynamic stressing on the plate interface, likely accentuating the triggering of slow slip that occurred following the Kaikoura earthquake. Accretionary prisms characterized by extremely low seismic velocities may enhance the generation of tsunami earthquakes and dynamic triggering of slow slip events observed in the northern Hikurangi and other subduction margins.

Plain Language Summary In this study, we discovered an unusually long duration (up to 8 minutes) of ground shaking near Gisborne, on the east coast of the North Island of New Zealand during the magnitude 7.8 Kaikoura earthquake in 2016, using data from accelerometer, GPS and ocean bottom pressure sensors. This is arguably the longest duration of long-period ground shaking ever documented from similar magnitude 7–8 earthquakes worldwide. To resolve why this occurred, we use numerical simulations of seismic wave propagation during the Kaikoura earthquake to show that the unusually long ground shaking near Gisborne was caused by the presence of large-scale (approximately 150,000 cubic kilometers) body of sediments offshore and beneath the northeastern North Island. This long-duration shaking was also responsible for triggering a large slow slip event on the Hikurangi subduction zone offshore Gisborne, over 600 km away from the Kaikoura earthquake. Our result has important local and global implications for ground shaking hazard in areas with similar geological characteristics to those in the northeastern North Island, and improves understanding of processes that can trigger slow slip events and earthquakes on subduction zones.

1. Introduction

It has been long recognized that sedimentary basins amplify earthquake-induced ground motions and increase the duration, often referred to as a “basin effect” (Bard & Bouchon, 1985; Day et al., 2008; Furumura & Hayakawa, 2007; Olsen et al., 2006; Pitarka et al., 2015; Singh et al., 1988). An analogy commonly used to describe the basin effect is shaking a bowl of jelly during which a less consolidated material (jelly) is more

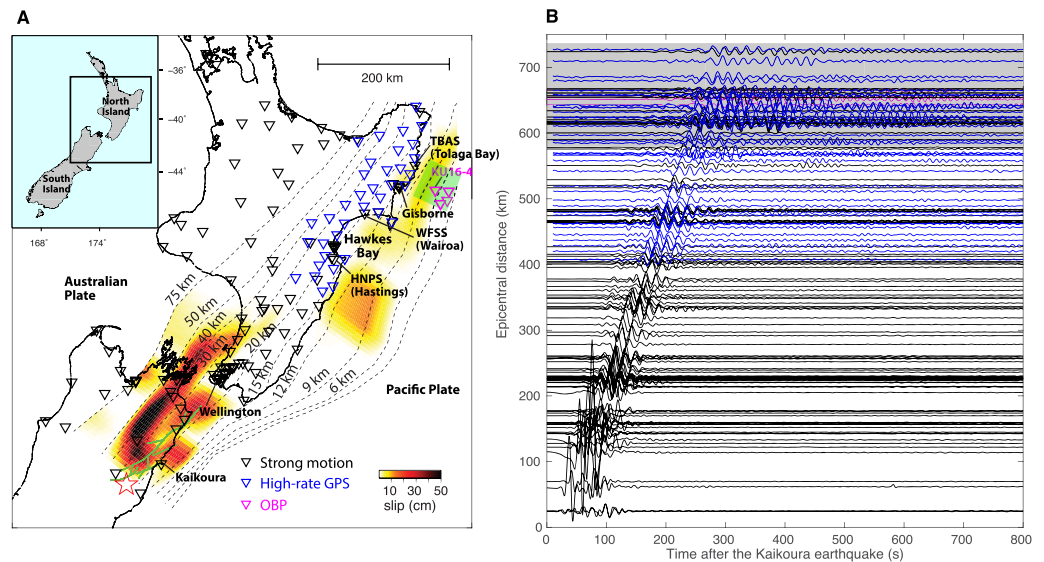


Figure 1. Long durations of long-period ground motions in the northeastern North Island of New Zealand during the $M7.8$ Kaikoura earthquake. (a) Map of the study region. Background color shows the total slip on the Hikurangi subduction interface over the year following the Kaikoura earthquake estimated from inversions of geodetic data (Wallace et al., 2018). The inverted triangles show the locations of strong-motion (black), high-rate GPS (blue), and ocean bottom pressure sensors (pink). The star and green lines correspond to the epicenter of the Kaikoura earthquake and the traces of the surface ruptures (Hamling et al., 2017), respectively. Dashed contours indicate depth (in kilometers) to the subduction interface. Green rectangle corresponds to the inferred source area of the 1947 $M_w 7.1$ tsunami earthquake (Bell et al., 2014). (b) Seismic record sections showing the vertical component of particle velocities band-pass-filtered between 10 and 100 s. Strong motion (black), high-rate GPS (blue), and OBP (pink) waveforms are shown. All the traces are scaled by the same value. Gray shade corresponds to the region where significantly longer durations of long-period ground motions are observed. OBP = ocean bottom pressure.

susceptible to stronger and longer-duration shaking than the surrounding stiffer bedrock (the bowl). The resonance period of amplified and prolonged ground motions in a basin largely depends on the size and depth of a basin as well as the impedance contrast between the less consolidated material and the bedrock. For example, the well-studied ~ 100 -km-wide and ~ 4 -km-deep Kanto basin underneath Tokyo has a resonance period of 7–12 s (Furumura & Hayakawa, 2007; Koketsu et al., 2009), whereas the Valley of Mexico underneath Mexico City extending ~ 20 km across and ~ 0.5 km deep shows a resonance period of 2–3 s (Cruz-Atienza et al., 2016). The excitation of these long-period waves within sedimentary basins poses serious hazard and risk in populated cities. For example, the basin effect led to serious damage to Mexico City during the 1985 $M8.1$ Michoacan earthquake (Singh et al., 1988) and severe damage of oil storage tanks during the 2003 $M8.0$ Tokachi-oki (Japan) earthquake (Koketsu et al., 2005).

Less understood is the basin effect that may occur in low seismic-velocity accretionary prisms, overlying subducted oceanic crust along subduction margins. Numerical simulations and observational data have identified the existence of amplified seismic waves and long duration of ground motions in accretionary prisms (Furumura et al., 2008; Gomberg, 2018; Guo et al., 2016; Nakamura et al., 2015; Noguchi et al., 2013; Shapiro et al., 2000). For example, long-period (> 10 s) ground motions lasting up to ~ 200 s have been reported in the Nankai trough region in southwestern Japan (Nakamura et al., 2015), indicating that a basin effect can also occur at ocean floors along subduction margins. Due to the only relatively recent development of off-shore monitoring systems, the full nature of a basin effect along many subduction margins is not well understood.

2. Observation of Anomalously Long Duration of Ground Motions Captured by on-Shore and off-Shore Sensors

We identified long-period ground motions lasting longer than 450 s due to an unusually strong basin effect in the North Island of New Zealand induced by seismic wave propagation from the $M7.8$ Kaikoura earthquake ~ 600 km away (Figure 1). This earthquake lasted ~ 90 s during which it ruptured a complex network of

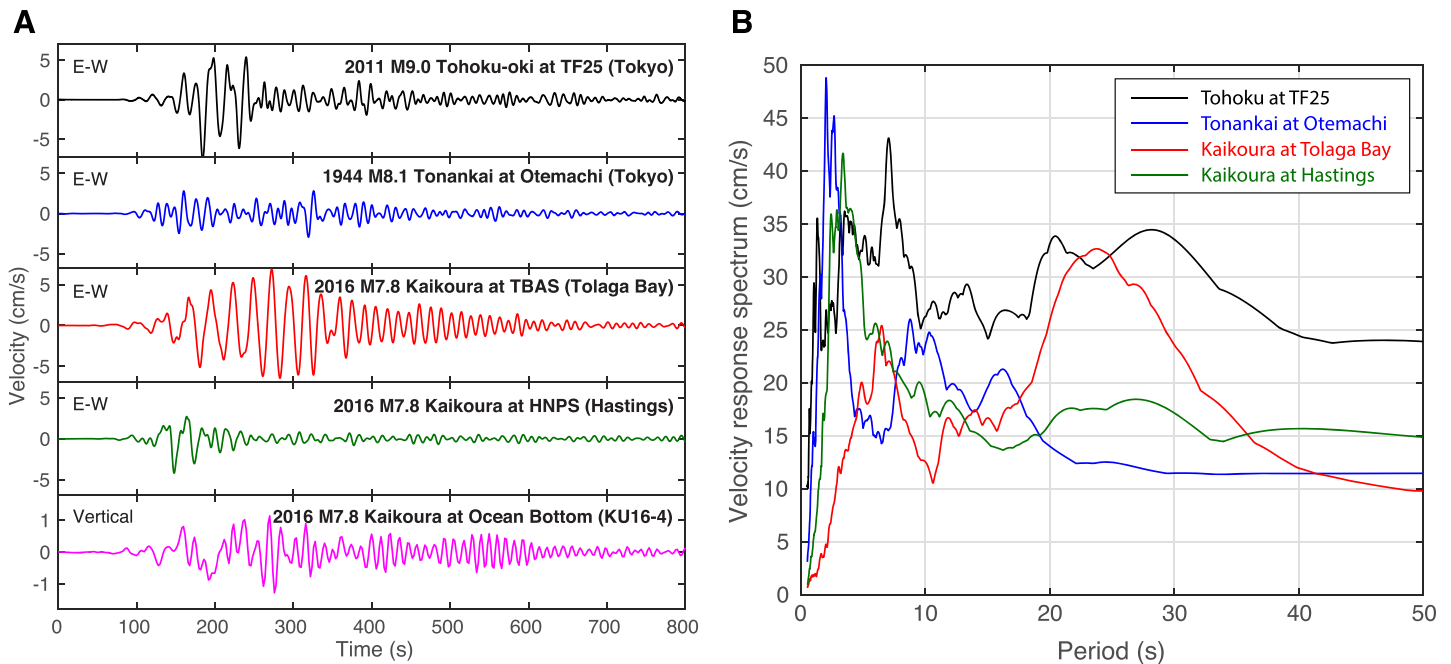


Figure 2. Long-duration ground motions due to the Kaikoura earthquake compared to ground motions recorded at the center of the Kanto basin (Tokyo) during megathrust earthquakes. (a) Horizontal component of velocity band-pass-filtered between 10 and 100 s. Time of each trace is shifted to roughly align the onset of large-amplitude signals. (b) Velocity response spectrum at the corresponding stations assuming a damping coefficient of 0.05. The geometrical mean of the response spectra of two horizontal components is shown. The ground motions at Tolaga Bay due to the Kaikoura earthquake show large wave excitation around the period of 20–30 s. The M9 Tohoku-oki earthquake waveform shows a large peak around the same period range due to the source effect (b).

crustal faults extending over a 150-km length in the northern South Island (Hamling et al., 2017; Holden et al., 2017; Kaiser et al., 2017; Kaneko et al., 2017; Wang et al., 2018). We collected a unique combination of onshore and offshore seismological and geodetic sensor data available during the Kaikoura earthquake, including those from ocean bottom pressure (OBP) sensors, high-rate onshore Global Navigation Satellite Systems data, and onshore strong-motion seismological stations (Figure 1a; see supporting information for data processing; Aster et al., 2013; Colosimo et al., 2011; Dow et al., 2009; Grapenthin et al., 2018; Herring et al., 2006; Hino et al., 2014; Polster et al., 2009; Webb, 1998). Kaikoura earthquake waveforms captured by these sensors reveal that the ground motions lasted 100–150 s in most of the North Island except in the

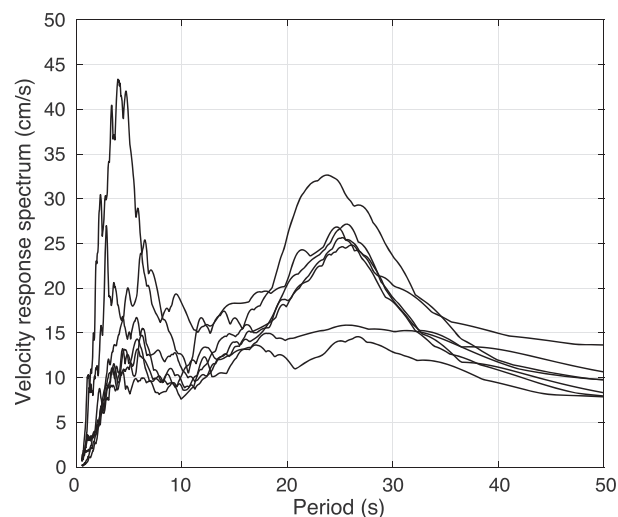


Figure 3. Velocity response spectra at strong motion stations in the northeastern North Island. A damping coefficient of 0.05 is assumed. A large excitation of ground motions occurs in the period range of 20–30 s.

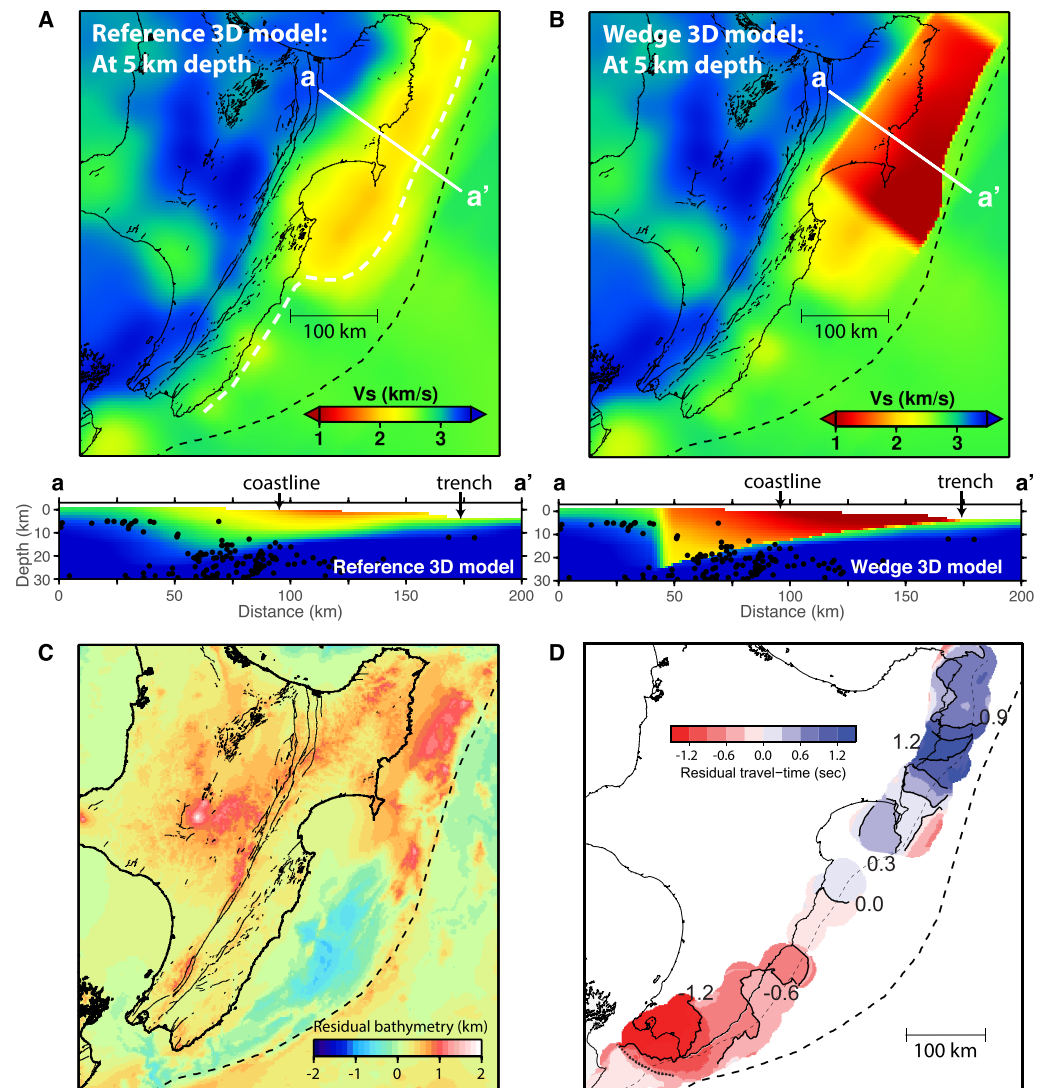


Figure 4. Three-dimensional velocity models used to simulate the observed long duration of ground motions. (a) Map of shear wave velocity at 5-km depth in the reference 3-D model (Eberhart-Phillips et al., 2015, 2017). White dashed line indicates the approximate boundary of resolution in the tomographic model (Eberhart-Phillips et al., 2015, 2017). Cross-sectional view along $a-a'$ is shown in the panel below. Black dots indicate background $M > 3$ seismicity in New Zealand's GeoNet catalog. (b) Map of shear wave velocity at 5-km depth in the revised model (referred to as wedge 3-D model). A large-scale, low-velocity wedge is added to the reference 3-D velocity model. The depth extent of the low-velocity wedge is defined by the region above the plate interface (Williams et al., 2013). (c) Map of residual bathymetry from Bassett and Watts (2015). (d) P wave traveltime anomalies estimated from onshore recordings of active-source marine seismic surveys (Bassett et al., 2014).

northeastern region (including the coastal city of Gisborne) where the apparent duration increases by a factor of 3 or more (>450 s; Figure 1b).

These >450 -s-duration onshore and offshore waveforms in the northeastern North Island are some of the longest durations of long-period (>10 s) ground motions ever recorded at similar epicentral distances for comparable, large earthquakes. In comparison to waveforms recorded in the Kanto basin due to the 1944 $M8.1$ Tonankai earthquake (at a comparable epicentral distance), the Kaikoura earthquake waveform at Tolaga Bay clearly shows stronger and longer duration of long-period ground motions (Figure 2a). The dominant excitation period at Tolaga Bay is in the range of 20–30 s (Figure 2b), 2–3 times longer than the resonance period of the Kanto basin. Many strong-motion, high-rate GPS and offshore OBP stations in this region reveal similar features in the waveforms (Figures 2a and 3). These unique waveforms imply that the

low-velocity accretionary prism extending both onshore and offshore the northeastern North Island is larger in size and thicker than the well-studied Kanto basin.

The region of the extremely long durations of Kaikoura earthquake ground motions is also the site of numerous slow slip events that have been reported here over the last ~15 years (Wallace et al., 2012). At the northern Hikurangi margin, shallow (<15 km depth) and short-duration (2–3 weeks) slow slip events recur every ~2 years, on average. The most recent, large slow slip event in this region is thought to have been triggered by passing seismic waves from the Kaikoura earthquake (Wallace et al., 2017; Figure 1a). Prolonged ground motions above the accretionary prism suggest that there was also a long duration of dynamic stressing on the plate interface, which can promote the triggering of slow slip (Wallace et al., 2017; Wei et al., 2018). In addition, the rupture velocity of the 1947 M_w 7.1 tsunami earthquake (which caused an unusually large tsunami for this earthquake magnitude) in this region, off the coast of Gisborne (Figure 1a), as inferred from seismic and tsunami data, is anomalously slow (~0.3 km/s; Bell et al., 2014), implying the presence of low-velocity materials in the source region. Therefore, understanding the cause of the extremely long duration ground motions is also relevant for understanding the possible role that elastic properties of the outer forearc and the plate boundary play in the generation of dynamically triggered slow slip events and tsunami earthquakes.

3. Origin of Long-Duration Ground Motions

We aim to reproduce the long duration of Kaikoura earthquake ground motions over 700 km to the northeast of the earthquake, using numerical simulations of seismic wave propagation which incorporate 3-D velocity and attenuation models of New Zealand (Eberhart-Phillips et al., 2015, 2017; referred to as the reference model in this study) and local topography and bathymetry. In the reference model, the offshore velocity is constrained by onshore-offshore data from marine air gun shots recorded at onshore stations (Eberhart-Phillips et al., 2017). A zone of lower velocities (both V_p and V_s) in the overriding plate extends along the Hikurangi margin (yellow color in Figure 4a), which has been interpreted as East Coast allochthon (Eberhart-Phillips et al., 2017) or Neogene accretionary margin sediments (Sutherland et al., 2009) overlying the subducted oceanic crust. The low-velocity zone extending down to the plate interface is characterized by 30–40% slower wave speeds compared to the surrounding stiffer rocks elsewhere in the North Island (Figure 4a).

We simulate seismic wave propagation resulting from the Kaikoura earthquake using open-source seismic wave propagation software SPECFEM3D (Komatitsch & Vilotte, 1998; Komatitsch et al., 2004). The computational domain is 1,200 km by 600 km at the Earth surface, extends to 400 km depth, and includes local topography and bathymetry. The mesh contains 4.7 million spectral elements with the average spacing between Gauss-Lobatto-Legendre node points at the Earth surface at 250 m. The minimum values of V_p , V_s , and density are 1.7 km/s, 0.98 km/s, and 1.7 g/cm³, respectively. Ocean water is not included in the computational mesh. To simulate realistic Kaikoura earthquake waves, we use a source model developed previously (Holden et al., 2017, Model A in their study) that fits local strong motion and geodetic (InSAR and GPS) data. A different source model (Wang et al., 2018) predicts similar amplitude and duration of ground motions throughout New Zealand, as was demonstrated by Wei et al. (2018). Each numerical simulation takes 12 hr on 256 cores on New Zealand's NeSI supercomputing cluster, and the seismic waves are numerically resolved down to a period of 2.5 s.

To quantify the misfits between observed and simulated ground motions, we calculate the following two quantities at each station: (i) the maximum amplitude of three-component waveforms, $|\mathbf{v}|_{\max}$, band-pass-filtered between 10 and 100 s, and (ii) ground motion duration defined here as the sum of time intervals over which the magnitude of velocity is larger than 20% of the peak value, $|\mathbf{v}| \geq 0.2|\mathbf{v}|_{\max}$ (see Figure 5a). Although a lower threshold (e.g., 10%) should more accurately reflect the true ground motion duration, relatively high noise in some high-rate GPS stations contaminates the duration estimates. In contrast, setting a higher threshold (e.g., 30%) excludes dominant coda waves (e.g., Figure 5a) that should be included in the duration estimate. The dependence of the choice of a duration threshold on the results will be discussed in section 4.

Simulated Kaikoura earthquake waves based on the reference model reproduce the amplitudes and durations of long-period (>10 s) ground motions in most of the North Island with the exception of the northeastern region (Figure 5). The low-velocity zone present in the reference model (Figure 4a) acts as a

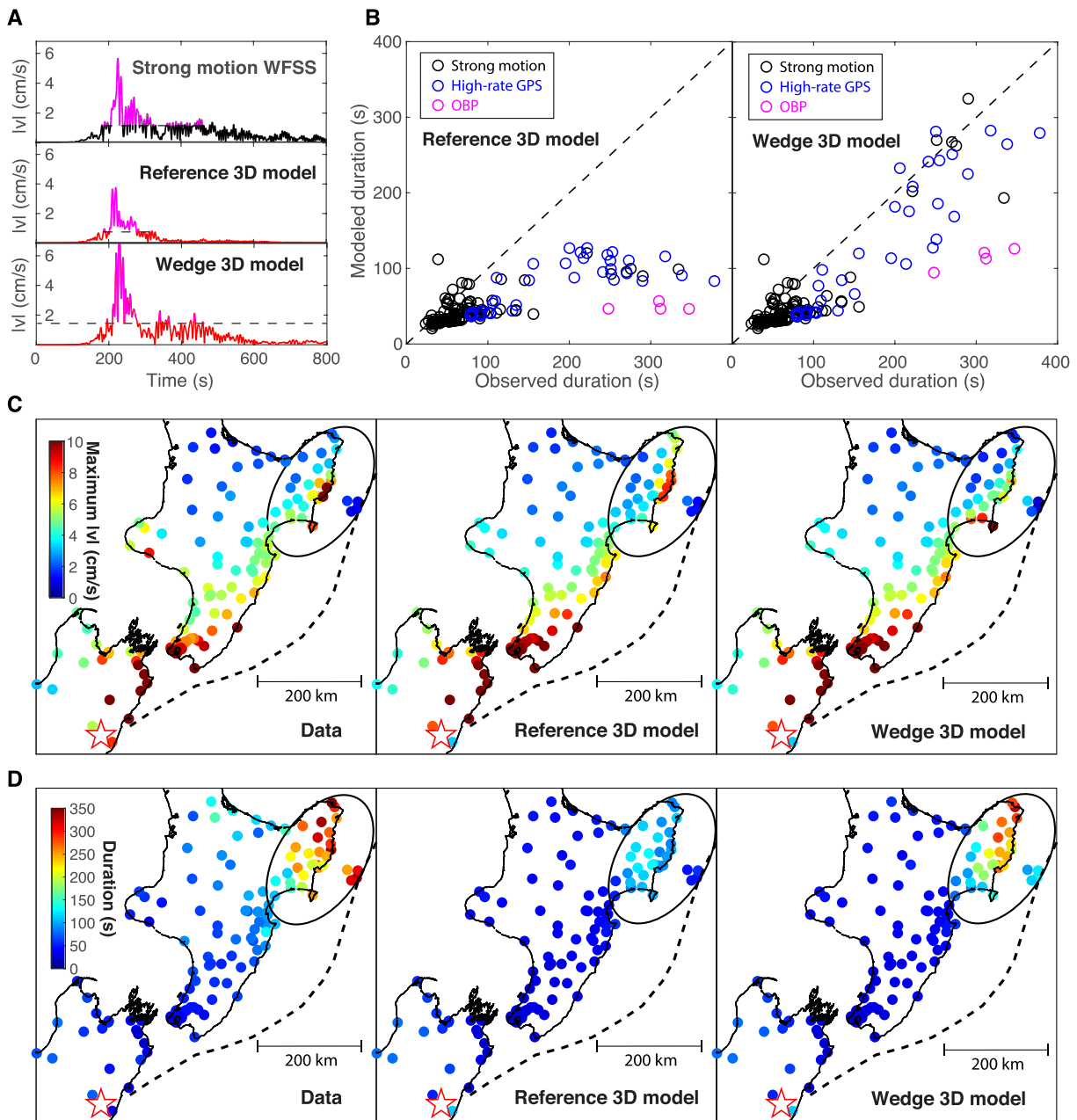


Figure 5. Modeling of long-period ground motions due to the Kaikoura earthquake. (a) The magnitude of three-component ground velocities $|\mathbf{v}|$ filtered between 10 and 100 s at a representative station for data (black) and synthetics (red) using the reference 3-D model and wedge 3-D model. The pink color corresponds to the time period over which $|\mathbf{v}|$ is greater than 20% of the maximum value, which is defined here as the duration of ground motions. (b) Comparisons between observed and computed durations using the reference 3-D model and wedge 3-D model. (c) Spatial characteristics of observed and modeled maximum $|\mathbf{v}|$. (d) Spatial characteristics of observed and modeled durations. The black contour outlines the region with a strong basin effect. OBP = ocean bottom pressure.

waveguide, trapping the seismic energy and inducing a basin effect along the Hikurangi margin to some degree. However, the extremely long durations of ground motions in the northeastern North Island are not captured by the synthetic seismograms (Figures 5b and 5d). Differences in observed and modeled durations are seen in all three components across a number of stations and are not limited to a particular component of motion (Figure 6). To match the long-duration ground motions observed, the low-velocity zone along the east coast must be characterized by even lower seismic wave speeds and/or higher impedance contrast than the reference model suggests.

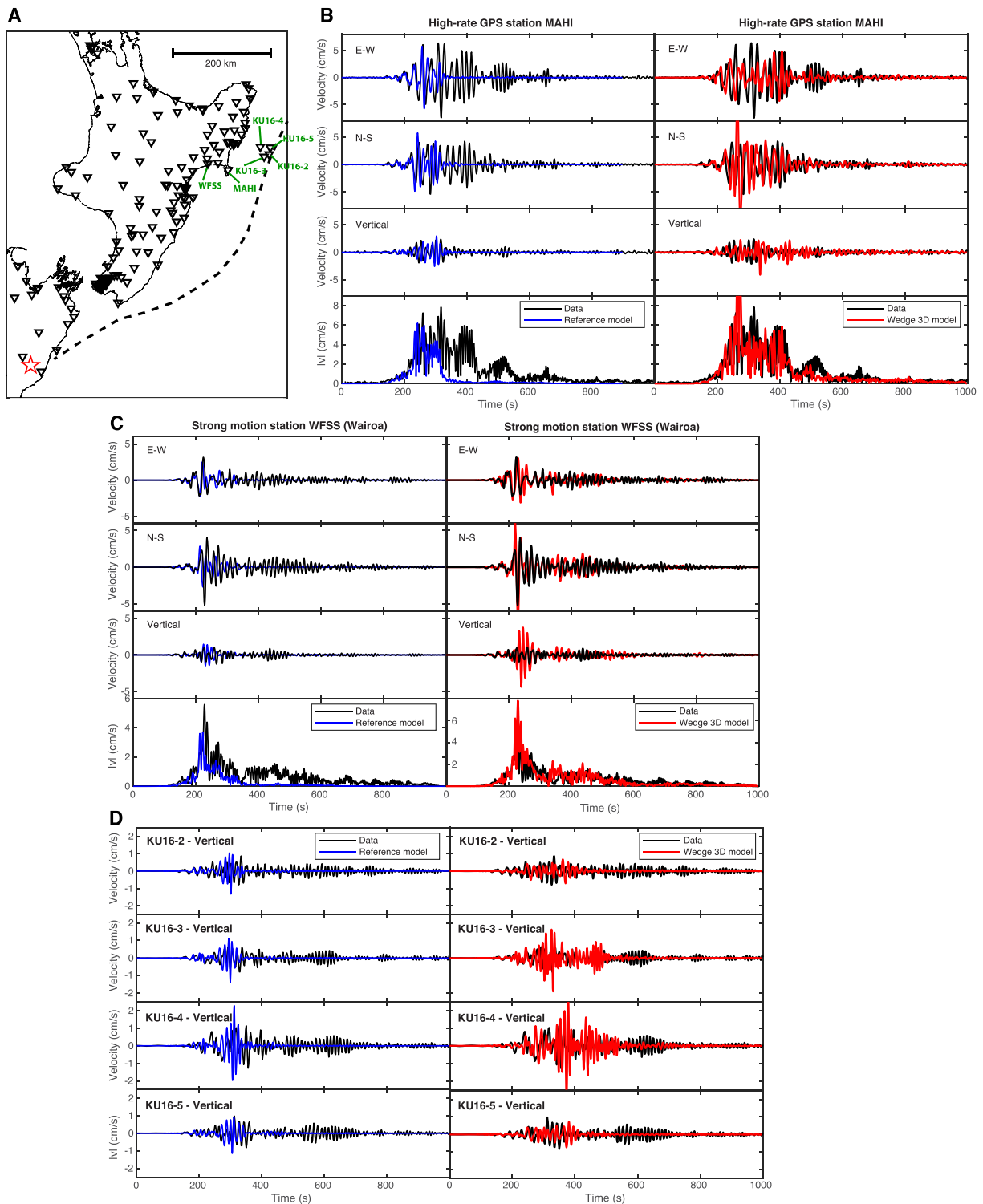


Figure 6. Comparison of observed and synthetic waveforms at selected stations. (a) Map showing the location of these stations. (b) Comparison between observed and computed waveforms at GPS station MAHI using the reference 3-D model and wedge 3-D model. (c) Comparison between observed and computed waveforms at strong-motion station WFSS. (d) Comparison between observed and computed waveforms at four ocean bottom pressure stations.

To explain the observations, we revise the reference 3-D model by adding a wedge characterized by low seismic wave speeds that increase the impedance contrast (Figure 4b). We consider a total of 22 models of a low-velocity wedge with the V_p and V_s ranging from 50% to 90% of the reference model (i.e., 10% to 50% reduction in the V_p and V_s), its trench-parallel length ranging from 180 to 300 km and the average trench-normal width ranging from 130 to 220 km. Following a widely used assumption that quality factors are linearly related to the seismic wave speeds (Olsen et al., 2003), we also modify the attenuation models (both Q_p and Q_s) within the wedge by the same factor as in the seismic wave speeds. To suppress reflections of seismic waves at the lateral boundaries of the wedge, which were not observed, a cosine taper with the length of 20 km is applied to all the boundaries except at the base of the wedge marked by the Hikurangi subduction interface (Figure 4b). By analyzing amplitude and duration misfits for different wedge models, we find that the ground motion duration is sensitive to whether the station is located within or far from the low-velocity wedge. We discuss the preferred model referred to as the “wedge 3-D model,” which is obtained by iteratively adjusting the dimensions and seismic wave speeds within the low-velocity wedge via comparisons of the observed and simulated durations of ground motions and which leads to the smallest misfit between observed and modelled ground motion durations.

With respect to the reference model, the seismic wave speeds (both V_p and V_s) in the wedge 3-D model are reduced by $\sim 40\%$ within the low-velocity wedge extending from Hawke's Bay to East Cape (Figure 4b). The depth profile of the average wave speeds within the low-velocity wedge is shown in Figure S2. The spatial extent of the low-velocity wedge (210 km by 140 km) is constrained by the region in which the long durations of ground motions are observed. Unlike the reference model, the wedge 3-D model extends the region of low velocities to depth ($V_s \sim 2$ km/s at 10-km depth; Figure 4b), creating a strong impedance contrast at the plate interface between the low-velocity wedge and stiffer subducted crust and further enhancing the basin effect.

A simulation based on the wedge 3-D model better replicates the extremely long durations of the ground motions observed in the northeastern North Island (Figures 5b–5d and 6 and Table S1). The durations within the low-velocity wedge are comparable to those observed and, on average, ~ 3 times longer than those in the reference 3-D model (Figure 5d). Although the wedge 3-D model does not capture observed large peak amplitudes along the coast (Figure 5c), the overall misfit of the peak amplitudes within and around the low-velocity wedge is comparable to that for the reference 3-D model (Figure S3 and Table S1), suggesting that these two models explain the overall peak amplitudes equally well. The long duration of ground motions is caused by reverberating surface waves (both Love and Rayleigh) within the low-velocity wedge (Figure 7). Due to the strong basin effect, the prolonged ground motions last more than 450 s from the first arrival of shear waves (Figure 6). The durations of ground motions at offshore OBP stations are still underestimated in our simulation (Figures 5b and 6), indicating that a better offshore velocity model is needed to explain the data.

Long durations of ground motions in the northeastern North Island are also found for smaller-magnitude earthquakes. Despite their smaller magnitudes and shorter source durations, the ground motions last up to 300 s, a factor of >3 longer than in other regions of the North Island with equivalent source-receiver distances (Figures S4–S6). Although the durations of ground motions for smaller-magnitude events are shorter than those for the Kaikoura earthquake, the pattern of the ground motion durations remains the same (Figures S4–S6), indicating that the underlying mechanism is related to the Earth structure and not due to local seismic source. In addition, the long durations of ground motions are observed for on-land earthquake-station paths (Figure S4), suggesting that water reverberation phases between ocean surface and seafloor (Yue et al., 2017) alone cannot explain the observations. Furthermore, the lack of long-duration ground motions in coastal regions south of Hawke's Bay (Figure 1) observed during the Kaikoura earthquake also precludes the ocean phase as the cause of long-duration ground motions in the northeastern North Island. Moreover, the patterns of ground motion durations for different frequencies remain qualitatively similar (Figure S7), supporting the conclusion that the long durations are caused by the low-velocity wedge.

4. Discussion and Conclusions

4.1. Sensitivity to the Choice of an Amplitude Threshold in Duration Definition

In this study, the duration of ground motions is defined as the sum of time intervals over which the magnitude of velocity is larger than 20% of the peak value. Since the choice of the threshold is somewhat arbitrary, we consider different amplitude thresholds and compare the results. Ground motion durations increase with decreasing threshold, as expected (Figure S8). However, the spatial patterns of both observed and modeled

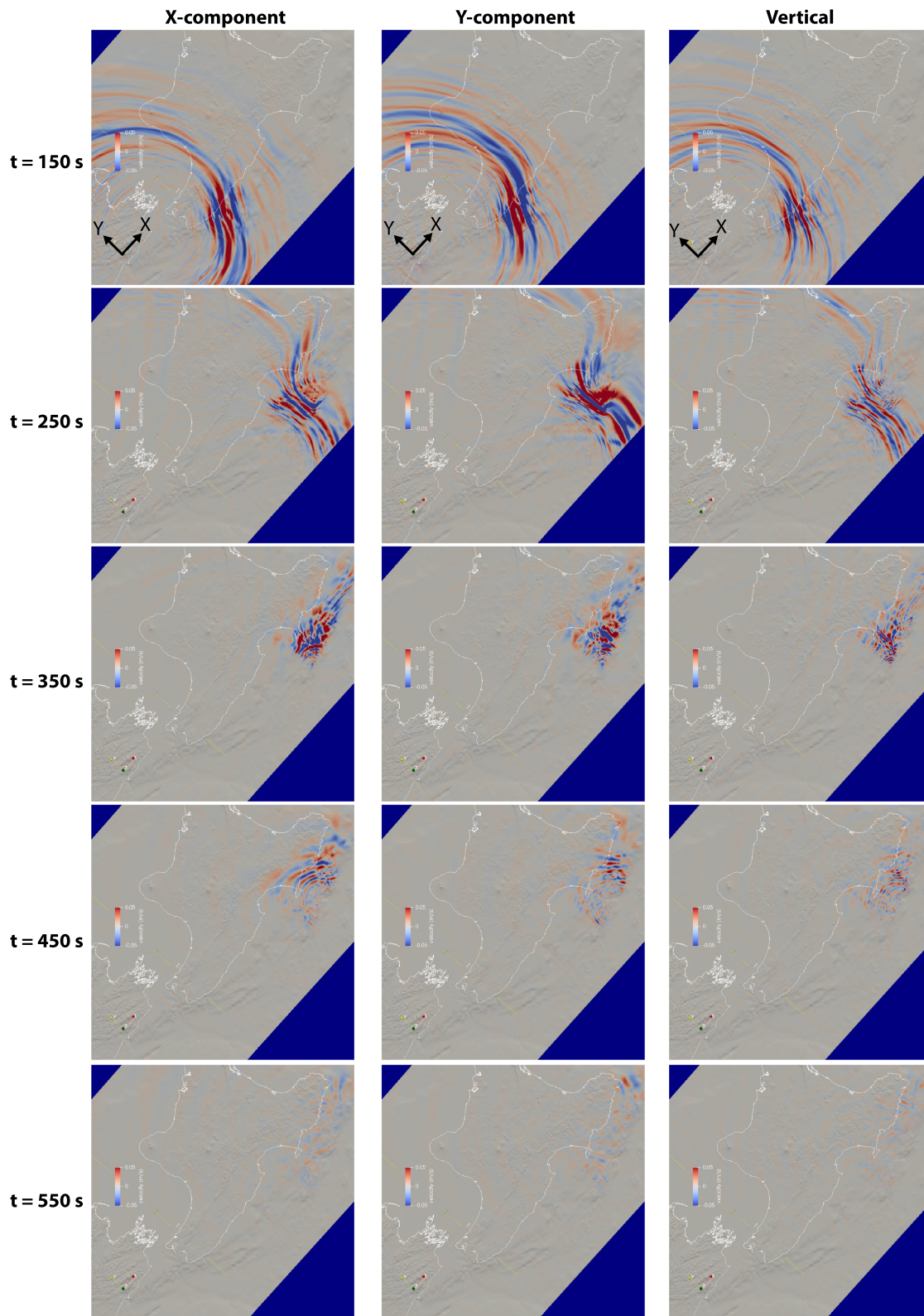


Figure 7. Snapshots of simulated seismic wave propagation with the wedge 3-D model. The color corresponds to ground velocities (in the scale of ± 5 cm/s) for the period range of 3 s and longer. The azimuths of X and Y axes are 40° and 310° from north, respectively. The source model of the Kaikoura earthquake (Model A in Holden et al., 2017) is used. The region within and around the low-velocity wedge in the northeastern North Island experiences long-duration ground shaking due to reverberating surface waves.

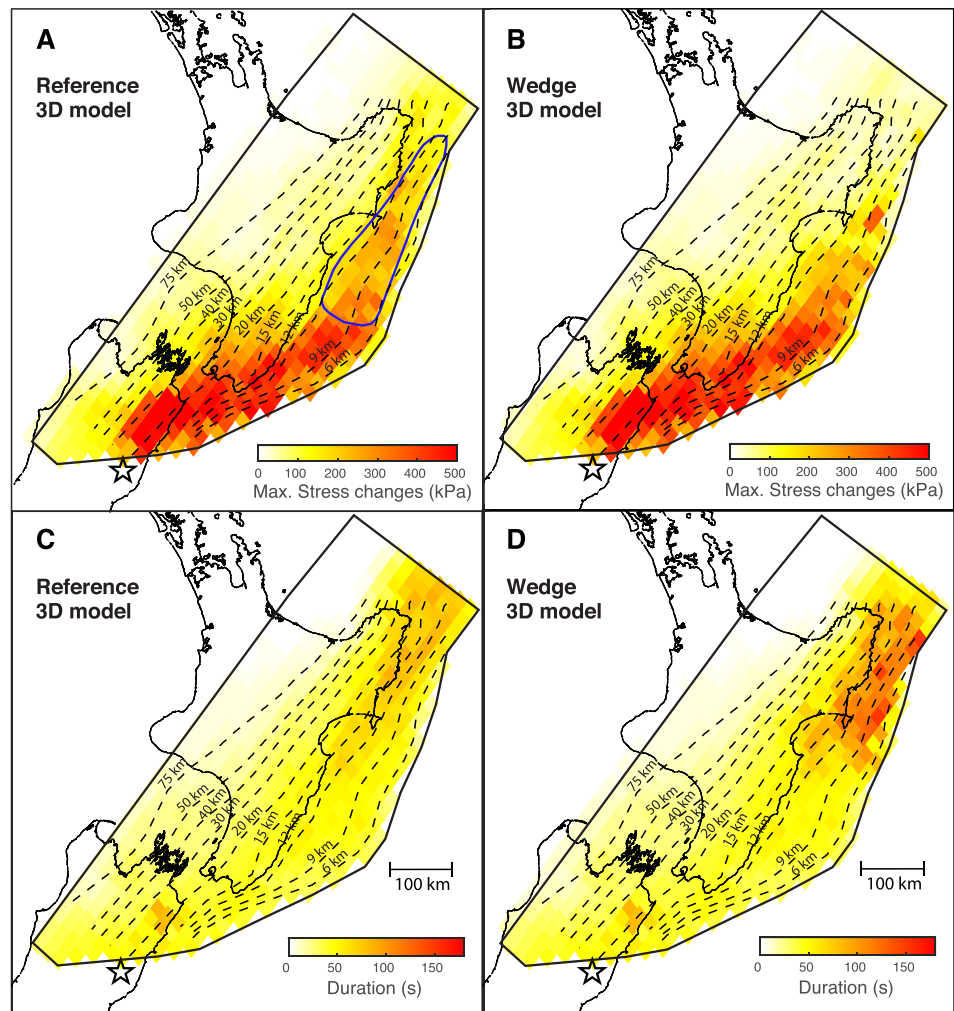


Figure 8. Dynamic stress changes on the Hikurangi subduction interface induced by the Kaikoura earthquake. The peak amplitude of positive dynamic stressing on the plate interface using (a) the reference 3-D model and (b) the wedge 3-D model. (c, d) The corresponding duration of positive dynamic stressing >10 kPa. The blue contour outlines triggered shallow slow slip events (Wallace et al., 2017).

durations remain qualitatively similar for different threshold values (Figure S8). In particular, we find that, regardless of the choice of a threshold, the wedge 3-D model better reproduces the observed duration than the reference 3-D model does (Figure S8).

4.2. Model Limitations

Several important simplifications are made in characterizing the low-velocity wedge. First, in the wedge 3-D model, both the V_p and V_s are reduced by the same factor with respect to the reference model. Since ground motion depends more on the V_s structure than the V_p one, we test the sensitivity of V_p on the ground motion durations by considering a wedge model with the reduction in the V_s alone. We find that a wedge model with the reduction in the V_s alone slightly underpredicts the observed ground motion durations but can still explain the data better than the reference model does (Figure S9 and Table S1). Therefore, the V_p values in the wedge 3-D model are not well constrained by the Kaikoura earthquake data alone. Second, we assume that the low-velocity zone simply extends down to the plate interface (Figure 4b). To assess whether the data can resolve seismic wave speeds at depths, we consider a case where the low-velocity zone is confined within the top 5 km of the overlying crust (Figure S10). Compared to the wedge 3-D model, this model reproduces the observed ground motion amplitude and durations equally well (Figure S10 and Table S1). This means that it is difficult to resolve the depth to the base of the low-velocity zone with the Kaikoura earthquake data alone, although there is no evidence for such a sharp seismic-velocity boundary anywhere else within

the overlying crust. Third, the actual velocity structure is likely more heterogeneous than the one currently assumed, which would increase the ground motion durations due to the scattering of seismic waves even at long periods.

In order to validate the wedge 3-D model, we compare the depth profiles of wave speeds to those reported in previous studies. Average V_p values within the upper plate in offshore Gisborne estimated from recent active-source studies (Barker et al., 2018; Bassett et al., 2014) lie between the V_p values of the reference 3-D model and the wedge 3-D model (Figure S2). As noted above, V_p values in the wedge 3-D model are not well constrained, and hence the discrepancy is not surprising. V_s models for this region from active-source studies do not exist. However, V_s in the top 600 m within the low-velocity wedge is in good agreement with V_s measured in situ using Logging While Drilling at an International Ocean Discovery Program site in the middle of our study area (Site U1519) during the recent Integrated Ocean Drilling Program Expedition 372 (Wallace et al., 2019), validating the V_s in the wedge 3-D model for the top 600 m (Figure S2). The agreement also indicates that an additional, superficial sedimentary layer is not required to explain the long-period Kaikoura earthquake data. While the proposed low-velocity wedge is likely too simplistic, our results suggest that a large-scale ($\sim 30,000$ km²), thick (> 5 km) low-velocity zone is needed to explain the observations.

4.3. Implications for Dynamic Triggering of Slow Slip Events

Previous studies suggested enhanced dynamic triggering of a shallow slow slip event due to the passing Kaikoura earthquake waves interacting with a low-velocity, accretionary wedge (Wallace et al., 2017). The extremely long duration of ground motions observed in the northern Hikurangi will lead to a longer duration of dynamic stressing on the plate interface, which can further promote the triggering of slow slip events (Wallace et al., 2017; Wei et al., 2018). To quantify this effect, we compute time-dependent stress changes on the Hikurangi subduction interface using the same wave propagation code. We compute time-dependent stress perturbations filtered between periods of 3 and 200 s, which are resolved into normal and shear stresses on the subduction interface (Williams et al., 2013). We report dynamic Coulomb stress changes on the Hikurangi subduction interface assuming an effective coefficient (King et al., 1994) of friction of 0.1. Duration of the dynamic stress changes is defined here as the sum of time intervals over which the dynamic stress changes are > 10 kPa.

Compared to the reference velocity model, the wedge 3-D model induces approximately 3 times longer durations of dynamic stressing on the plate interface (compared to previous estimates; Wallace et al., 2017) while the maximum amplitudes remain similar (Figure 8). Different parameterizations of a low-velocity wedge discussed above lead to similar increases in dynamic-stressing durations on the plate interface (Figure S11). Enhanced triggering potential provided by such a strong basin effect suggests that slow slip events in the northern Hikurangi might be commonly triggered by regional large ($M > 7$) earthquakes (Koulali et al., 2017) including those from the Kermadec-Tonga subduction zone.

4.4. Relation to Local Geology

The presence of a large, low-velocity wedge is consistent with inferences from previous geological and geophysical studies. Low-velocity, upper crustal materials (relative to areas further south, in terms of V_p) have been inferred from residual traveltimes at the offshore northern Hikurangi margin (Bassett et al., 2014; Figure 4d). Thick sedimentary units of the East Coast Basin in northern Hawke's Bay can be identified in the stratigraphic cross sections constructed from a number of petroleum exploration wells (Figure S12; Mazengarb & Speden, 2000; Francis et al., 2004; Lee et al., 2011). From an exploration well near Mahia Peninsula (OPOUTAMA-1), Miocene sedimentary rocks are found at 4- to 5-km depths (Francis et al., 2004; Mazengarb & Speden, 2000). This suggests a lack of basement rocks older than Miocene in at least the upper 4–5 km of the overlying crust in northern Hawke's Bay (Francis et al., 2004; Figure S12), which is thicker than the well-studied Kanto basin. Moreover, the Eocene Wanstead Formation may form an effective regional seal in the offshore East Coast Basin, leading to fluid overpressure in the underlying formation (Burgreen-Chan et al., 2016), contributing to the presence of a low-velocity wedge at even greater depths. In contrast, older basement rocks are exposed near the coast in locales south of Hawke's Bay and are situated at shallower depths relative to further north (Figure S12).

4.5. Implications for Other Subduction Forearcs

The location of the inferred low-velocity wedge lies above a region of previously documented shallow slow slip events and tsunami earthquakes (Figure 1a). The low-velocity wedge also coincides with a region of high residual bathymetry (Bassett & Watts, 2015; Figure 4c), representing areas where the seafloor is more

elevated relative to the average elevation along the subduction zone; this could represent the presence of oversteepened topography (e.g., a larger wedge taper angle) or elevated topography related to subduction of features such as seamounts (Bassett & Watts, 2015) or a combination of the two. In turn, a larger wedge taper angle could be explained by either (a) lower cohesion of the rocks forming the outer wedge (Dahlen, 1990) or (b) a higher coefficient of friction on the plate boundary (Fagereng, 2011). If the former interpretation (low cohesion) is correct, this could be related to the presence of fluid-rich, underconsolidated sediments composing much of the northern wedge (Bassett et al., 2014). Thus, if taper angle, residual bathymetry, and low seismic velocities are a result of linked processes (such as a low cohesion wedge), this implies that other subduction forearcs with high residual bathymetry (such as Java and Nicaragua) may also be more susceptible to tsunami earthquake generation (Bassett & Watts, 2015; Fan et al., 2017) and dynamic triggering of shallow slow slip events.

4.6. Implications for Seismic Hazard in the Northeastern North Island

The strong basin effect in the northeastern North Island poses significant seismic hazard and risk for large infrastructures, such as high-rise buildings, dams, and bridges. While the region overlying the low-velocity wedge is relatively rural (the town of Gisborne has a population of 37,000), our results suggest that this region is prone to severe, long-period ground shaking due to large earthquakes, which needs to be taken into consideration for future building designs. In addition, our work suggests that low-velocity wedges at northern Hikurangi and elsewhere may be more susceptible to dynamic triggering of tsunami earthquakes due to the strong basin effect. A better characterization of this low-velocity wedge via high-resolution, onshore and offshore tomographic studies will enable better understanding of the impact of this feature on seismic and tsunami hazards and slow slip processes in this region.

Acknowledgments

We thank Takashi Furumura for providing us the digitized waveforms of the M8.1 Tonankai earthquake. We also thank Shin-ichi Sakai for sharing the MeSO-net waveform of the M9 Tohoku-oki earthquake. We also thank Kim Olsen, an anonymous reviewer and the Associate Editor for their comments that helped us improve the manuscript. Numerical simulations were run on the New Zealand eScience Infrastructure (NeSI) high-performance computing facilities. The strong-motion waveform data used in this study are publically available and can be downloaded from New Zealand's GeoNet website (<https://www.geonet.org.nz>). The processed high-rate GPS and OBP data are available online (at ftp://ftp.gns.cri.nz/pub/ykaneko/KaikouraEQ_Data/). OBP data were acquired through the New Zealand Ministry for Business, Innovation, and Employment (MBIE) Endeavour fund and through MBIE Strategic Science Investment Fund (SSIF), contracted to NIWA, for ship time on the RV Tangaroa (TAN1709 and TAN1607).

References

- Aster, R. C., Borchers, B., & Thurber, C. H. (2013). *Parameter estimation and inverse problems* (2nd ed.). Amsterdam: Elsevier Academic Press.
- Bard, P. Y., & Bouchon, M. (1985). The two-dimensional resonance of sediment-filled valleys. *Bulletin of the Seismological Society of America*, 75(2), 519–541.
- Barker, D. H. N., Henrys, S., Caratori, T. F., Barnes, P. M., Bassett, D., Todd, E., & Wallace, L. M. (2018). Geophysical constraints on the relationship between seamount subduction, slow slip, and tremor at the north Hikurangi subduction zone, New Zealand. *Geophysical Research Letters*, 45, 12,804–12,813. <https://doi.org/10.1029/2018GL080259>
- Bassett, D., Sutherland, R., & Henrys, S. (2014). Slow wavespeeds and fluid overpressure in a region of shallow geodetic locking and slow slip, Hikurangi subduction margin, New Zealand. *Earth and Planetary Science Letters*, 389, 1–13.
- Bassett, D., & Watts, A. B. (2015). Gravity anomalies, crustal structure, and seismicity at subduction zones: 1. Seafloor roughness and subducting relief. *Geochemistry, Geophysics, Geosystems*, 16, 1508–1540. <https://doi.org/10.1002/2014GC005684>
- Bell, R., Holden, C., Power, W., Wang, X., & Downes, G. (2014). Hikurangi margin tsunami earthquake generated by slow seismic rupture over a subducted seamount. *Earth and Planetary Science Letters*, 397, 1–9.
- Burgreen-Chan, B., Meisling, K. E., & Graham, S. (2016). Basin and petroleum system modelling of the East Coast basin, New Zealand: A test of overpressure scenarios in a convergent margin. *Basin Research*, 28(4), 536–567.
- Colosimo, G., Crespi, M., & Mazzoni, A. (2011). Real-time GPS seismology with a stand-alone receiver: A preliminary feasibility demonstration. *Journal of Geophysical Research*, 116, B11302. <https://doi.org/10.1029/2010JB007941>
- Cruz-Atienza, V. M., Tago, J., Sanabria-Gómez, J. D., Chaljub, E., Etienne, V., Virieux, J., & Quintanar, L. (2016). Long duration of ground motion in the paradigmatic valley of Mexico. *Scientific reports*, 6, 38807.
- Dahlen, F. A. (1990). Critical taper model of fold-and-thrust belts and accretionary wedges. *Annual Review of Earth and Planetary Sciences*, 18(1), 55–99.
- Day, S. M., Graves, R., Bielak, J., Dreger, D., Larsen, S., Olsen, K. B., & Ramirez-Guzman, L. (2008). Model for basin effects on long-period response spectra in Southern California. *Earthquake Spectra*, 24(1), 257–277.
- Dow, J. M., Neilan, R. E., & Rizos, C. (2009). The international GNSS service in a changing landscape of global navigation satellite systems. *Journal of Geodesy*, 83(3–4), 191–198.
- Eberhart-Phillips, D., Bannister, S., & Reyners, M. (2017). Deciphering the 3-D distribution of fluid along the shallow Hikurangi subduction zone using P- and S-wave attenuation. *Geophysical Journal International*, 211(2), 1032–1045.
- Eberhart-Phillips, D., Reyners, M., & Bannister, S. (2015). A 3D QP attenuation model for all of New Zealand. *Seismological Research Letters*, 86, 1655–1663. <https://doi.org/10.1785/0220150124>
- Fagereng, A. (2011). Wedge geometry, mechanical strength, and interseismic coupling of the Hikurangi subduction thrust, New Zealand. *Tectonophysics*, 507(1–4), 26–30.
- Fan, W., Bassett, D., Jiang, J., Shearer, P. M., & Ji, C. (2017). Rupture evolution of the 2006 Java tsunami earthquake and the possible role of splay faults. *Tectonophysics*, 721, 143–150.
- Francis, D., Bennett, D., & Courtney, S. (2004). Advances in understanding of onshore East Coast Basin structure, stratigraphic thickness and hydrocarbon generation. *New Zealand Petroleum Conference Proceedings*, 1–20.
- Furumura, T., & Hayakawa, T. (2007). Anomalous propagation of long-period ground motions recorded in Tokyo during the 23 October 2004 M_w 6.6 Niigata-ken Chuetsu, Japan, earthquake. *Bulletin of the Seismological Society of America*, 97(3), 863–880.
- Furumura, T., Hayakawa, T., Nakamura, M., Koketsu, K., & Baba, T. (2008). Development of long-period ground motions from the Nankai Trough, Japan, earthquakes: Observations and computer simulation of the 1944 Tonankai (M_w 8.1) and the 2004 SE Off-Kii Peninsula (M_w 7.4) earthquakes. *Pure and Applied Geophysics*, 165, 585–607.
- Gomberg, J. (2018). Cascadia onshore-offshore site response, submarine sediment mobilization, and earthquake recurrence. *Journal of Geophysical Research: Solid Earth*, 123, 1381–1404. <https://doi.org/10.1002/2017JB014985>

- Grapenthin, R., West, M., Tape, C., Gardine, M., & Freymueller, J. (2018). Single-frequency instantaneous GNSS velocities resolve dynamic ground motion of the 2016 M_w 7.1 Iniskin, Alaska, earthquake. *Seismological Research Letters*, 89(3), 1040–1048.
- Guo, Y., Koketsu, K., & Miyake, H. (2016). Propagation mechanism of long-period ground motions for offshore earthquakes along the Nankai trough: Effects of the accretionary wedge. *Bulletin of the Seismological Society of America*, 106(3), 1176–1197.
- Hamling, I. J., Hreinsdóttir, S., Clark, K., Elliot, J., Liang, C., Fielding, E., & Stirling, M. (2017). Complex multi-fault rupture during the 2016 M_w 7.8 Kaikōura earthquake, New Zealand. *Science*, 356, eaam7194. <https://doi.org/10.1126/science.aam7194>
- Herring, T. A., King, R. W., & McClusky, S. C. (2006). GAMIT reference manual. *GPS Analysis at MIT, release, 10*, 36.
- Hino, R., Inazu, D., Ohta, Y., Ito, Y., Suzuki, S., Iinuma, T., & Kaneda, Y. (2014). Was the 2011 Tohoku-Oki earthquake preceded by aseismic preslip? Examination of seafloor vertical deformation data near the epicenter. *Marine Geophysical Research*, 35, 181–190. <https://doi.org/10.1007/s11001-013-9208-2>
- Holden, C., Kaneko, Y., D'Anastasio, E., Benites, R., Fry, B., & Hamling, I. J. (2017). The 2016 Kaikōura earthquake revealed by kinematic source inversion and seismic wavefield simulations: Slow rupture propagation on a geometrically complex crustal fault network. *Geophysical Research Letters*, 44, 11,320–11,328. <https://doi.org/10.1002/2017GL075301>
- Kaiser, A., Balfour, N., Fry, B., Holden, C., Litchfield, N., Gerstenberger, M., & Gledhill, K. (2017). The Kaikōura (New Zealand) earthquake: Preliminary seismological report. *Seismological Research Letters*, 88, 727–739. <https://doi.org/10.1785/0220170018>
- Kaneko, Y., Fukuyama, E., & Hamling, I. J. (2017). Slip-weakening distance and energy budget inferred from near-fault ground deformation during the 2016 M_w 7.8 Kaikōura earthquake. *Geophysical Research Letters*, 44, 4765–4773. <https://doi.org/10.1002/2017GL073681>
- King, G. C. P., Stein, R. S., & Lin, J. (1994). Static stress changes and the triggering of earthquakes. *Bulletin of the Seismological Society of America*, 84, 935–953.
- Koketsu, K., Hatayama, K., Furumura, T., Ikegami, Y., & Akiyama, S. (2005). Damaging long-period ground motions from the 2003 M_w 8.3 Tokachi-oki, Japan earthquake. *Seismological Research Letters*, 76(1), 67–73.
- Koketsu, K., Miyake, H., & Tanaka, Y. (2009). A proposal for a standard procedure of modeling 3-D velocity structures and its application to the Tokyo metropolitan area, Japan. *Tectonophysics*, 472(1–4), 290–300.
- Komatitsch, D., Liu, Q., Tromp, J., Suss, P., Stidham, C., & Shaw, J. H. (2004). Simulations of ground motion in the Los Angeles basin based upon the spectral-element method. *Bulletin of the Seismological Society of America*, 94(1), 187–206.
- Komatitsch, D., & Vilotte, J. P. (1998). The spectral element method: An efficient tool to simulate the seismic response of 2D and 3D geological structures. *Bulletin of the Seismological Society of America*, 88, 368–392.
- Kouali, A., McClusky, S., Wallace, L., Allgeyer, S., Tregoning, P., D'Anastasio, E., & Benavente, R. (2017). Slow slip events and the 2016 Te Araroa M_w 7.1 earthquake interaction: Northern Hikurangi subduction, New Zealand. *Geophysical Research Letters*, 44, 8336–8344.
- Lee, J. M., Bland, K. J., Townsend, D. B., & Kamp, P. J. J. (2011). Geology of the Hawke's Bay area, Institute of Geological and Nuclear Sciences 1: 250,000 geological map 8.1 sheet+ 93 p. GNS Science, Lower Hutt. OpenURL.
- Mazengarb, C., & Speden, I. G. (2000). *Geology of the Raukumara area* (Vol. 6). Lower Hutt, New Zealand: Institute of Geological & Nuclear Sciences.
- Nakamura, T., Takenaka, H., Okamoto, T., Ohori, M., & Tsuboi, S. (2015). Long-period ocean-bottom motions in the source areas of large subduction earthquakes. *Scientific reports*, 5, 16648.
- Noguchi, S., Maeda, T., & Furumura, T. (2013). FDM simulation of an anomalous later phase from the Japan Trench subduction zone earthquakes. *Pure and Applied Geophysics*, 170(1–2), 95–108.
- Olsen, K. B., Day, S. M., & Bradley, C. R. (2003). Estimation of Q for long-period (> 2 sec) waves in the Los Angeles basin. *Bulletin of the Seismological Society of America*, 93(2), 627–638.
- Olsen, K. B., Day, S. M., Minster, J. B., Cui, Y., Chourasia, A., Faerman, M., & Jordan, T. (2006). Strong shaking in Los Angeles expected from southern San Andreas earthquake. *Geophysical Research Letters*, 33, L07305. <https://doi.org/10.1029/2005GL025472>
- Pitarka, A., Al-Amri, A., Pasyanos, M. E., Rodgers, A. J., & Mellors, R. J. (2015). Long-period ground motion in the Arabian Gulf from earthquakes in the Zagros Mountains thrust belt. *Pure and Applied Geophysics*, 172(10), 2517–2532.
- Polster, A., Fabian, M., & Villinger, H. (2009). Effective resolution and drift of Paroscientific pressure sensors derived from long-term seafloor measurements. *Geochemistry, Geophysics, Geosystems*, 10, Q08008. <https://doi.org/10.1029/2009GC002532>
- Shapiro, N. M., Olsen, K. B., & Singh, S. K. (2000). Wave-guide effects in subduction zones: Evidence from three-dimensional modeling. *Geophysical Research Letters*, 27(3), 433–436.
- Singh, S. K., Mena, E. A., & Castro, R. (1988). Some aspects of source characteristics of the 19 September 1985 Michoacan earthquake and ground motion amplification in and near Mexico City from strong motion data. *Bulletin of the Seismological Society of America*, 78(2), 451–477.
- Sutherland, R., Stagpoole, V., Uruski, C., Kennedy, C., Bassett, D., Henrys, S., et al. (2009). Reactivation of tectonics, crustal underplating, and uplift after 60 Myr of passive subsidence, Raukumara Basin, Hikurangi-Kermadec fore arc, New Zealand: Implications for global growth and recycling of continents. *Tectonics*, 28, TC5017. <https://doi.org/10.1029/2008TC002356>
- Wallace, L. M., Barnes, P., Beavan, J., Van Dissen, R., Litchfield, N., Mountjoy, J., & Pondard, N. (2012). The kinematics of a transition from subduction to strike-slip: An example from the central New Zealand plate boundary. *Journal of Geophysical Research*, 117, B02405. <https://doi.org/10.1029/2011JB008640>
- Wallace, L. M., Hreinsdóttir, S., Ellis, S., Hamling, I. J., D'Anastasio, E., & Denys, P. (2018). Triggered slow slip and afterslip on the southern Hikurangi subduction zone following the Kaikōura earthquake. *Geophysical Research Letters*, 45, 4710–4718. <https://doi.org/10.1002/2018GL077385>
- Wallace, L. M., Kaneko, Y., Hreinsdóttir, S., Hamling, I. J., Peng, Z., Bartlow, N., & Fry, B. (2017). Large-scale dynamic triggering of shallow slow slip enhanced by overlying sedimentary wedge. *Nature Geoscience*, 10(10), 765.
- Wallace, L. M., Saffer, D. M., Barnes, P. M., Pecher, I. A., Petronotis, K. E., LeVay, L. J., & Wu, H. Y. (2019). Expedition 372B/375 methods. *Proceedings of the International Ocean Discovery Program*, 372B/375. <https://doi.org/10.14379/iodp.proc.372B375.102.2019>
- Wang, T., Wei, S., Shi, X., Qiu, Q., Li, L., Peng, D., & Barbot, S. (2018). The 2016 Kaikōura earthquake: Simultaneous rupture of the subduction interface and overlying faults. *Earth and Planetary Science Letters*, 482, 44–51.
- Webb, S. C. (1998). Broadband seismology and noise under the ocean. *Reviews of Geophysics*, 36(1), 105–142.
- Wei, M., Kaneko, Y., Shi, P., & Liu, Y. (2018). Numerical modeling of dynamically triggered shallow slow slip events in New Zealand by the 2016 M_w 7.8 Kaikōura earthquake. *Geophysical Research Letters*, 45, 4764–4772. <https://doi.org/10.1029/2018GL077879>
- Williams, C. A., Eberhart-Phillips, D., Bannister, S., Barker, D. N. H., Henrys, S., Reyners, M., & Sutherland, R. (2013). Revised interface geometry for the Hikurangi subduction zone, New Zealand. *Seismological Research Letters*, 84(6), 1066–1073.
- Yue, H., Castellanos, J. C., Yu, C., Meng, L., & Zhan, Z. (2017). Localized water reverberation phases and its impact on backprojection images. *Geophysical Research Letters*, 44, 9573–9580. <https://doi.org/10.1002/2017GL073254>